EARTHQUAKE ENGINEERING AND STRUCTURAL DYNAMICS
Earthquake Engng. Struct. Dyn. **28**, 1121–1141 (1999)

REAL-TIME HYBRID EXPERIMENTAL SYSTEM WITH ACTUATOR DELAY COMPENSATION AND ITS APPLICATION TO A PIPING SYSTEM WITH ENERGY ABSORBER

T. HORIUCHI[1,*], M. INOUE[1], T. KONNO[2] AND Y. NAMITA[1]

[1] *Mechanical Engineering Research Laboratory, Hitachi Ltd, 502 Kandatsu-machi, Tsuchiura-shi, Ibaraki-ken, 300-0013, Japan*

[2] *Tsuchiura Works, Hitachi Ltd, 603 Kandatsu-machi, Tsuchiura-shi, Ibaraki-ken, 300-0013, Japan*

SUMMARY

A real-time hybrid experimental method, in which output from an actuator-excited vibration experiment and response calculation are combined on-line and conducted simultaneously in real time, is being developed as a new seismic experimental method for structural systems. In real-time hybrid experiments, however, there is an inevitable actuator-response delay, which has an effect equivalent to negative damping. To solve this problem, a real-time hybrid experimental system (including an actuator-delay compensation method) was developed. And seismic experiments were conducted in order to demonstrate the advantages of this system. Experimental results obtained using the developed hybrid experimental system were compared with exact results obtained using shaking-table experiments, and it was found that the two experimental methods gave almost identical results. It can therefore be concluded that the structural response can be obtained precisely by using the developed hybrid experimental system. Comparison of these experiments showed the advantages of the hybrid experiments; that is, they are simple and economical. This is because the hybrid experiment requires only a small structure as the excitation model, while a shaking-table experiment must consider the whole structural system.

KEY WORDS: seismic experiment; hybrid experiment; pseudo-dynamic experiment; real time; hydraulic actuator; delay compensation

1. INTRODUCTION

The seismic response of a structural system is usually evaluated by using a shaking table. However, due to table-capacity limitations, shaking-table experiments for large-scale structures are sometimes difficult. As a solution to this problem, Hakuno *et al.*[1] proposed a seismic experimental method in which an actuator-excitation experiment on a part of a structural system is combined with vibration response calculations on a computer. This method has been developed and improved through various projects, which have been summarized by Iemura,[2] Takanashi *et al.*[3] and Mahin *et al.*[4] This method will be referred to here as a 'hybrid experiment'

* Correspondence to: T. Horiuchi, Mechanical Engineering Research Laboratory, Hitachi Ltd, 502 Kandatsu-machi, Tsuchiura-shi, Ibaraki-ken 300-0013, Japan

CCC 0098–8847/99/101121–21$17·50

Received 24 September 1998
Revised 17 March 1999

because it is a *hybrid* of actuator-excitation experiments and computer simulation. Note that the method is also referred to in various other ways such as *computer-actuator on-line experiment* or *pseudo-dynamic experiment*. In these experiments, a hydraulic actuator is generally used because it has a large exciting force.

Actuator excitation in hybrid experiments is usually conducted on an expanded time axis so that the structural response can be observed easily. However, when the response depends heavily on velocity because of damping, the excitation should be conducted in real time; in other words, the actuator excitation and the computer simulation should be conducted on a common time axis. The dynamic characteristics of hydraulic actuators, however, inevitably include a response delay, which is equivalent to negative damping in a real-time hybrid experiment. Therefore, the systems which have been developed for real-time experiments[1,5,6] could be applied only to the structures with a small stiffness or a large damping although these research efforts successfully showed the advantages of their various systems through demonstration experiments. To achieve a more flexible and practical experimental system which can be used for wider varieties of structural systems, we developed a method for delay compensation.[7] In this report, a description of hybrid experiments will be followed by an outline and discussions of the developed compensation method for experiments in real time. An example of seismic experiments for an actual system will also be shown.

2. OVERVIEW OF HYBRID EXPERIMENTS

A conceptual view of a hybrid experiment using the substructuring technique is shown in Figure 1. The original structure, of which the seismic response is of interest, is divided into two parts. One is actually modelled, and the model is excited with an actuator. We will call this part the 'structure under excitation'. The other part is modelled numerically and inputted to a computer. In the computer, the vibration response of the numerical model is calculated based on the following equation of motion:

$$\mathbf{M}\ddot{\mathbf{x}} + \mathbf{C}\dot{\mathbf{x}} + \mathbf{K}\mathbf{x} = \mathbf{f} + \mathbf{q} \tag{1}$$

where **M**, **C** and **K** are the mass, damping, and stiffness matrices, respectively, of the numerical model, **x** is a relative displacement vector, **f** is an external force vector, **q** is a reaction force vector generated at the boundary of the actual and the numerical models, and the overdots represent differentiation with respect to time. The reaction force vector **q** is formally written using the displacement at the boundary, x_b, as follows:

$$\mathbf{q} = \mathbf{q}(x_b, \dot{x}_b, \ddot{x}_b, \ldots) \tag{2}$$

Therefore, by repeating the following steps, the seismic response of the whole structure can be evaluated: (1) measure the reaction force **q** from the actuator-excitation experiment; (2) calculate the vibration response of the numerical model using the measured reaction-force vector **q** and the predetermined external-force vector **f**; and (3) excite the actual model based on the calculated vibration response **x**. This experimental method allows us to conduct seismic experiments economically by replacing part of the structure with a numerical model. The method also makes it possible to calculate seismic response for structures including a part that is difficult to model numerically. From equation (2), it can be understood that it is necessary to conduct the excitation

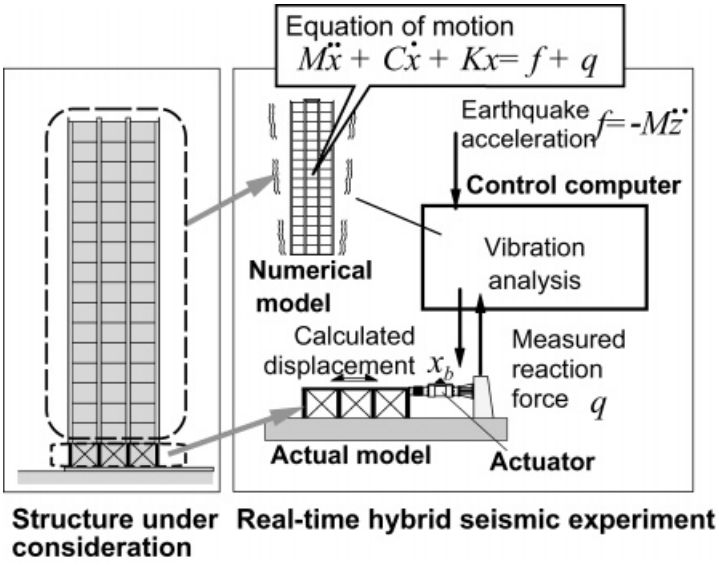

Figure 1. Conceptual view of hybrid experiment

experiment and the computer calculation on a common time axis (that is, in real time) if the reaction force depends largely on displacement derivatives with respect to time.

3. ACTUATOR-DELAY COMPENSATION

3.1. Dynamic characteristics of hydraulic actuators

Since applying the hybrid experimental method to a large-scale structure requires a large actuator-excitation force, hydraulic actuators are preferable in such cases. However, the dynamic characteristics of hydraulic actuators include a small but inevitable response delay. A representative example of this delay characteristic is shown in Figure 2, which compares the input signal and the resulting displacement. This response delay is equivalent to negative damping in a real-time hybrid experiment and this is explained as follows. Consider an experiment on a Single-Degree-Of-Freedom (SDOF) system, as shown in Figure 3(a), where a spring with a stiffness k is under excitation (as shown in Figure 3(b)). Let ω_0 and δt be the natural circular frequency of the SDOF system and the response delay time of the actuator, respectively, and assume the damping is zero for simplicity. The reaction force to be used for calculating, q, is proportional not to the calculated displacement of the mass x but to the actual excited displacement x''. When the system is in free vibration with displacement amplitude A, the calculated displacement x can be written as follows:

$$x = A \sin \omega_0 t \tag{3}$$

The actual excited displacement x'', then, becomes

$$x'' = A \sin(\omega_0 t - \omega_0 \delta t) \tag{4}$$

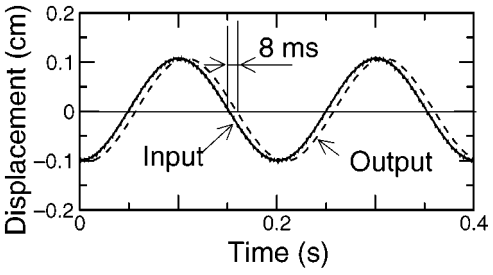

Figure 2. Time history of input and output signals for a hydraulic actuator

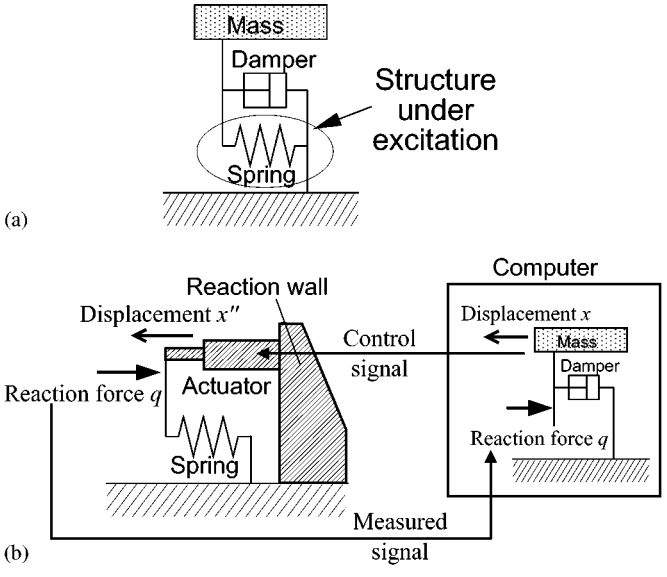

Figure 3. Real-time hybrid experiment for a single-degree-of-freedom system. (a) An SDOF system; (b) hybrid experiment

Therefore, by assuming that δt is small, the change in the total system energy per period, δE, becomes

$$\delta E = \oint q\,\mathrm{d}x = \int_0^T q\,\frac{\mathrm{d}x}{\mathrm{d}t}\,\mathrm{d}t = \int_0^T (kx'')\,\frac{\mathrm{d}x}{\mathrm{d}t}\,\mathrm{d}t$$

$$= \int_0^T kA\sin(\omega_0 t - \omega_0\delta t)\cdot A\omega\cos(\omega_0 t)\,\mathrm{d}t = \frac{1}{2}kA^2\cdot 2\pi\omega_0\delta t \tag{5}$$

where $T = 2\pi/\omega_0$. This means that the response delay of the actuator in real-time hybrid experiments causes the increase of the total energy. This energy increase is the same as that caused by equivalent negative damping c_{eq}; that is,

$$c_{\mathrm{eq}} = -k\delta t \tag{6}$$

If the negative damping is larger than the inherent structural damping, the response will diverge and the experiment will thus become impossible. Therefore, response delay time needs to be cancelled.

3.2. Method for compensating actuator delay

The developed compensation method predicts the displacement of the actuator after the actuator delay δt.[8] A schematic of this process is shown in Figure 4(a), where x, x', and x'' are the displacements *calculated* (by the computer), *predicted* (by the prediction subsystem), and *resulting* (caused by the actuator), respectively. By inputting the predicted value x' as a control signal to the actuator, the resulting displacement x'' becomes almost identical to the calculated one x, because the input signal occurs after the delay time. Since the prediction-calculation time needs to be small in order to accomplish real-time experiments, the following simple equation is used:

$$x' = \sum_{i=0}^{n} a_i x_i \tag{7}$$

where n is the order of prediction, x_0 is the present calculated displacement, x_i is the calculated displacement at $\delta t \times i$ units of time ago, and a_i constants are listed in Table I. In this equation, the predicted value x' was obtained by extrapolating an nth-order polynomial function based on present and n previous calculated values, as shown in Figure 4(b). As an example, the case when

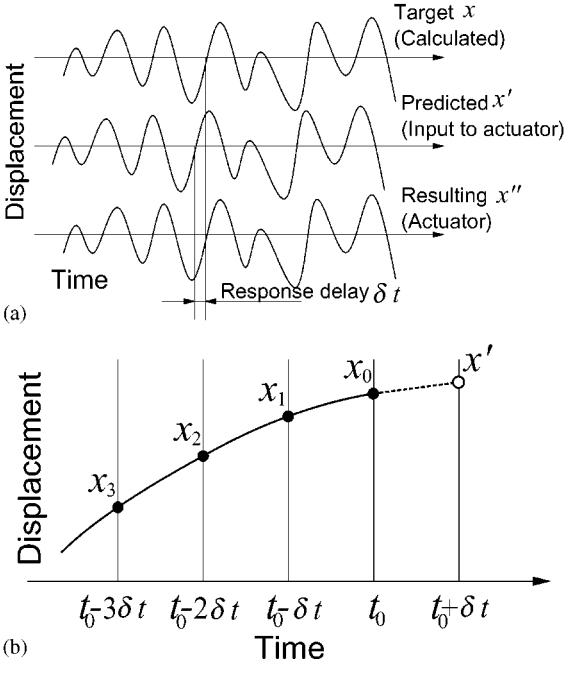

Figure 4. Schematic of prediction method (a) Displacement prediction for delay compensation; (b) calculation of predicted value x'

Table I. Constants in equation for prediction

Order n	a_0	a_1	a_2	a_3	a_4
0	1	–	–	–	–
1	2	− 1	–	–	–
2	3	− 3	1	–	–
3	4	− 6	4	− 1	–
4	5	− 10	10	− 5	1

$n = 1$ will be explained. The extrapolation function for $n = 1$ is a first-order (linear) function. This linear function with respect to time, $P(t)$, in which $P(t_0) = x_0$ and $P(t_0 - \delta t) = x_1$, can be written as

$$P(t) = (x_0 \cdot (t - \{t_0 - \delta t\}) - x_1 \cdot (t - t_0))/\delta t \tag{8}$$

The predicted displacement value at $t = t_0 + \delta t$ based on this function, x', can be calculated by substituting $t = t_0 + \delta t$ into equation (8) such that

$$x' = P(t_0 + \delta t) = 2x_0 - x_1 \tag{9}$$

This formula becomes identical to that in equation (7) and thus the a_i constants become as listed in Table I. Although only the case when $n = 1$ was discussed for simplicity, the a_i constants can be yielded in a similar manner for the other values of n.

3.3. Limitation of proposed method

Since a perfect prediction is impossible, some limitation must exist in application of such compensation as discussed above. This limitation will be discussed by considering an experiment on a single-degree-of-freedom model. By introducing the prediction subsystem on the SDOF experiment shown in Figure 3, the control signal to the actuator gains the predicted value x' instead of the calculated value x. Let the calculated vibration response x be a sinusoidal wave with a circular frequency of ω and an amplitude of A, such that $x = A \sin \omega t$. The actual-excited displacement x'' obtained through the prediction subsystem written in equation (7) and the actuator with the response delay of δt, therefore, becomes as follows:

$$x'' = \sum_{i=0}^{n} a_i \sin(\omega t - (i + 1)\omega \delta t) \tag{10}$$

By considering the fact that $\dot{x} = A\omega \cos \omega t$, the reaction force used in the calculation, q, can be written as follows:

$$q = kx'' = k_n^* x + c_n^* \dot{x} \tag{11}$$

where k_n^* and c_n^* are the apparent stiffness and damping, respectively, for the nth-order prediction, in which

$$k_n^*/k = \sum_{i=0}^{n} a_i \cos(i + 1)\omega \delta t, \qquad c_n^* \omega / k = - \sum_{i=0}^{n} a_i \sin(i + 1)\omega \delta t \tag{12}$$

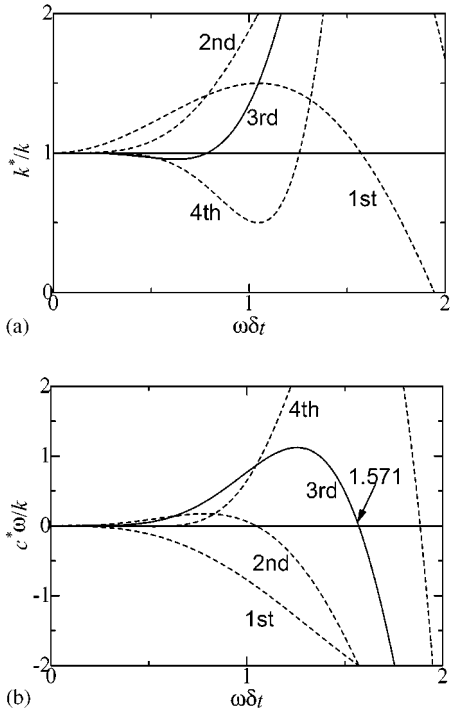

Figure 5. Variation of apparent additional stiffness and damping for $\omega\delta t$. (a) Apparent stiffness; (b) apparent damping

From equation (12), it is obvious that the apparent stiffness k_n^* and damping c_n^* are functions of $\omega\delta t$ as shown in Figures 5(a) and (b). The value k_n^*/k is almost equal to one and the value $c_n^*\omega/k$ is almost equal to zero and, therefore, this prediction is almost ideal when $\omega\delta t$ is small, although the prediction causes small variations both in stiffness and damping. It should be noted, however, that the damping becomes negative, and thus the calculation diverges, when the natural frequency of the structure considered is large or the actuator delay is large so that the value of $\omega\delta t$ is larger than a critical value that depends on the prediction depth n. This is the limitation of the developed compensation method. In the experiments discussed below, the third-order prediction, which is drawn with solid lines in Figures 5(a) and (b), will be used because it requires only a small calculation load and gives a large critical value of $\omega\delta t$ (1·571) for stable calculation.

As discussed above, the stability in calculation depends on the non-dimensional value $\omega\delta t$. It is obvious that each actuator has its own response delay, and therefore the frequency range for stable calculation is varied case by case (e.g. since an actuator with a large load capacity generally has a large response delay, only a low-frequency phenomenon can be simulated in such cases). It should be noted, however, that the following discussions, in which a few case of response delay will be adopted, can be generalized though the non-dimensional parameter $\omega\delta t$.

Although the results were obtained for an SDOF system, these can be easily expanded for Multiple-Degree-Of-Freedom (MDOF) systems through equation (1). An element of an MDOF numerical model is replaced by the actual model by making use of the hybrid experimental system. The characteristics of the actual model in calculation are the same as discussed above and,

therefore, the critical value for stable calculation is also the same. It should be noted that the highest natural frequency of the total structure must be treated as the excitation frequency ω in considering the calculation stability.[9]

3.4. Verification of the proposed compensation method

For verifying the compensation method discussed above, the compensation subsystem was constructed using a Digital Signal Processor (DSP) as shown in Figure 6(a) and the relationship between the input and output signals was investigated. We installed a modification function which modifies the prediction parameters so that the calculated displacement x and the resulting displacement x' become almost the same.[7] It should be noted that the delay time of actuators varies a little depending on the excitation frequency and amplitude. The modification function can cancel this change of the delay time. For these experiments, an electrical delay element was used instead of an actuator because the delay time was taken as an experimental parameter. The time step for calculation used in the DSP was 0·5 ms, which is sufficiently smaller than the delay time considered here.

The transfer function from input to output with the delay of 8 ms under the bandwidth white-noise input up to 20 Hz ($\omega\delta t = 1{\cdot}00$) was measured as shown in Figure 6(b). This delay of 8 ms is the same as that of the actuator shown in Figure 2 and used in the experiment discussed later. Although the amplitude and the phase fluctuate in high frequencies, an amplitude of unity and a phase of zero are obtained in the measuring frequency range. This compensation subsystem

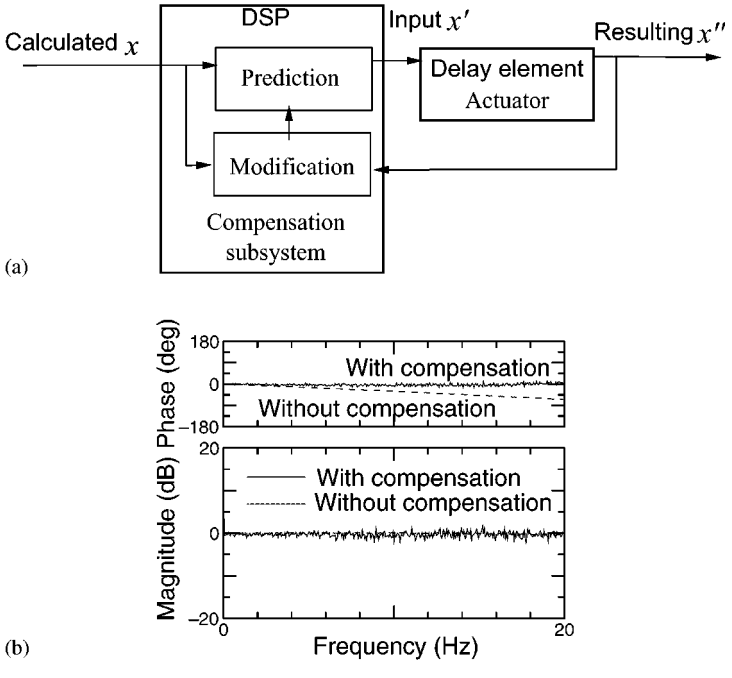

Figure 6. Verification of delay compensation subsystem. (a) Block diagram of compensation used in verification experiments; (b) transfer function of compensation subsystem with delay element

therefore has good characteristics even for a wide-band-frequency vibration which cannot actually take place in hybrid experiments.

4. EVALUATION OF DEVELOPED SYSTEM

4.1. Objectives

The following verification experiments were performed in order to demonstrate that seismic experiments on structural systems can be conducted precisely by using the developed system. Firstly, a hybrid experiment was conducted on a system whose characteristics were clearly known. Secondly, a numerical simulation was conducted under the same conditions as the hybrid experiment but the whole structural system was numerically modelled. Finally, the results of the experiment and the simulation were compared.

4.2. Experimental set-up

In an actual hybrid experiment, an actuator with a response delay excites the structure under excitation by following the control signal supplied by a control computer, then the reaction force induced in the structure, which is sometimes non-linear, is measured and the measured reaction force is fed back to the computer. However, the experiment was conducted using the system shown in Figure 7(a) instead. A DSP was used as a control computer for performing vibration

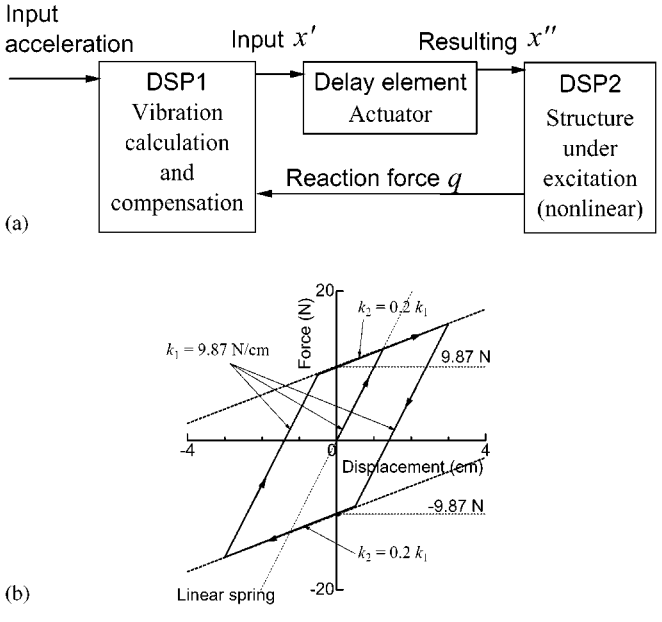

Figure 7. Experimental set-up for verifying a seismic experimental system. (a) Method of experiment; (b) numerical model of nonlinear elements

response calculation and compensation. This DSP will be referred to as DSP-1 below. The structure under excitation was replaced by another DSP (referred to as DSP-2 in the following) which outputs a simulated reaction force depending on a displacement input. The output follows a specific relationship programmed in the DSP shown in Figure 7(b). In addition, an actual actuator was simulated using an electronic delay element. By applying this set-up, the signals treated by the control computer become identical in the actual hybrid experimental system. The results obtained using this system will be called *Experimental results* in this section. The reason why the above experimental set-up was used is explained as follows. For verification of the developed system, the *exact* solution is desirable in order to know the error in the experimental results attributed to the experimental system. However, it is usually very difficult to make an exact numerical model of an actual structure because of inevitable complicated non-linearity; thus, an actual structure is not suitable for this experimental purpose. Therefore, the actual structure was replaced by the DSP-2, which can feed back the clearly modelled reaction force.

The experiments were performed under the following conditions. The time step for calculation and control used in DSP-1 was 0·5 ms (control frequency: 2 kHz). Since predicted displacement for the compensation was calculated with the calculated displacement for this time step, the discrepancy between the prediction time δt_p and the actual delay δt is at most 0·5 ms.

4.3. Experimental model

For simplicity, a linear single-degree-of-freedom model with a mass m of 1 kg, a natural frequency of 5 Hz, and a damping ratio ζ of 5 per cent are considered here. The systems used for experiments are the linear system mentioned and the system in which a linear spring is replaced by the non-linear element discussed in the following. The reaction force caused by the spring was simulated using the DSP-2 and the vibration response of the other part was calculated using DSP-1. The part simulated by DSP-2 will be called *the structure under excitation* in this section.

The non-linear element shown in Figure 7(b) is considered typical. The dotted line in the figure shows the characteristics of the linear spring discussed above. This element is a bilinear elasto-plastic spring (bilinear element), which is used to evaluate the vibration response for considering elasto-plastic deformation of structures. This element gives a smaller resonant frequency than that in a linear system and works as a damping element which dissipates vibration energy when the response is relatively large, while the natural frequency of a small displacement amplitude is identical to that of the linear system.

4.4. Response delay of the actuator

The response delay of the actuator was simulated using an electronic delay element as discussed above. Experiments with the 0-ms delay and the 8-ms delay were conducted to investigate the influence of the delay on the experimental results. The delay of 8 ms was selected according to the delay of an actual actuator (Figure 2). In addition, experiments with various delay times were also performed. It should be noted that this 8-ms delay is not exact but includes a small error because of the resolution of the delay element used.

4.5. Input acceleration

Two types of input acceleration were used in this experiment. One is sinusoidal sweep excitation, in which the excitation frequency is gradually varied with a constant amplitude. The

other is 5-period sinusoidal excitation of 5 Hz. The input amplitude was 494 or 987 cm/s^2. These amplitudes were selected so that the influence of non-linearity could be clearly observed and the dependency on the input amplitude could be investigated. Even though random excitation was not experimented here, the conclusions may be almost the same as our sinusoidal results because the structural response for random excitations is similar to that for sinusoidal excitations.

4.6. Numerical simulation to obtain exact solutions

Exact solutions to be compared with the experimental results were obtained as follows. The time-integral method used was the central difference algorithm. For the 5-period sinusoidal excitation, time step Δt was equal to 0·0032 s and the calculation period was 2 s. For the sweep excitation, the excitation frequency varied from 2·5 to 10 Hz in 100 steps on a logarithmic scale, and the response was calculated for 100 periods at each frequency and the maximum amplitude in the last period was taken as the solution.

4.7. Results

4.7.1. Linear system. Firstly, the results of the sweep excitation are shown in Figure 8(a) for delays of 0 and 8 ms. Since this model is linear, the results are shown only for the amplitude of

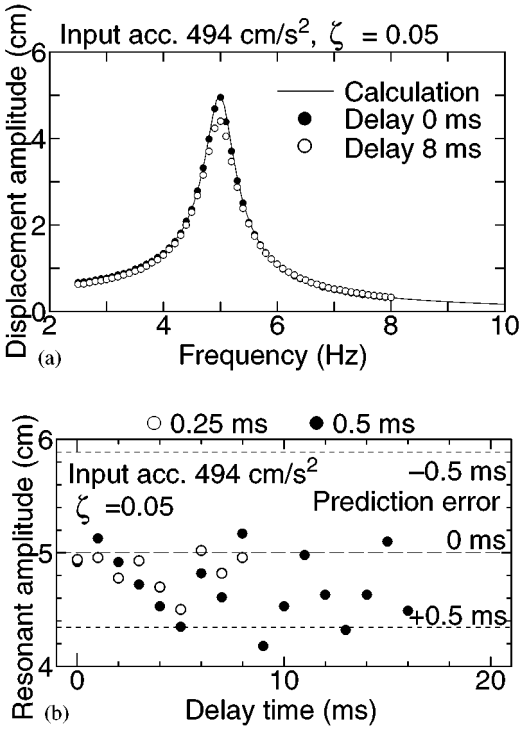

Figure 8. Results of sweep-excitation experiment on linear system. (a) Response curve of linear system; (b) resonant amplitude for delay time in linear system

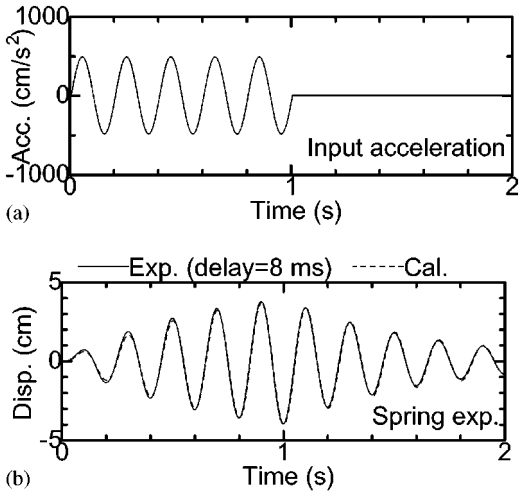

Figure 9. Response time history of linear system. (a) Input acceleration; (b) response time history

494 cm/s^2. Although experimental and calculation results are almost identical, it can be observed that the experimental results are a little smaller than the calculated ones around the resonant frequency (5 Hz) when $\delta t = 8$ ms. The relationship between the delay time and the maximum amplitude is shown in Figure 8(b). It can be seen that the maximum amplitudes do not vary monotonously for the delay but are scattered around the amplitude of 5 cm. This error may be caused by the fact that the predicted time δt_p was not exactly the same as the actual actuator delay δt. Since this error works as δt in equation (6), too large or too small a prediction causes positive or negative damping, respectively. In these experiments, the maximum error is the control period (that is, 0·5 ms) which is equivalent to the damping ratio error of 0·76 per cent. In Figure 8(b), the damping ratios (ζ) of 4·24 and 5·76 per cent, which are consistent with the prediction error of 0·5 ms, are also shown and the experimental data are dropped between the two lines. In addition, the experimental results with time step of 0·25 ms are also shown in Figure 8(b); this condition is equivalent to the prediction resolution of 0·25 ms. The fact that the discrepancy becomes small in this case supports the above discussions.

As for the results obtained from the 5-period sinusoidal excitation, the response with the delay of 8 ms under the 494-cm/s^2 5-Hz and 5-period excitation is shown in Figure 9. This figure shows that the calculated and experimental results are in good agreement, even though small discrepancies are found which may be caused by the additional damping resulting from the prediction error.

4.7.2. Bilinear element. The system shown in Figure 3 (where the linear spring is replaced by a bilinear element) is discussed here. The results obtained in the sweep-excitation experiments with 0- and 8-ms delay are shown in Figure 10(a), in which the experimental results are close to the calculation results. However, it should be noted that the experimental data are slightly smaller than the calculated data around the frequency giving the maximum amplitude. As previously explained, this phenomenon can be explained in terms of the additional damping caused by prediction error. As observed in Figure 10(b), in which the resonant curves calculated with

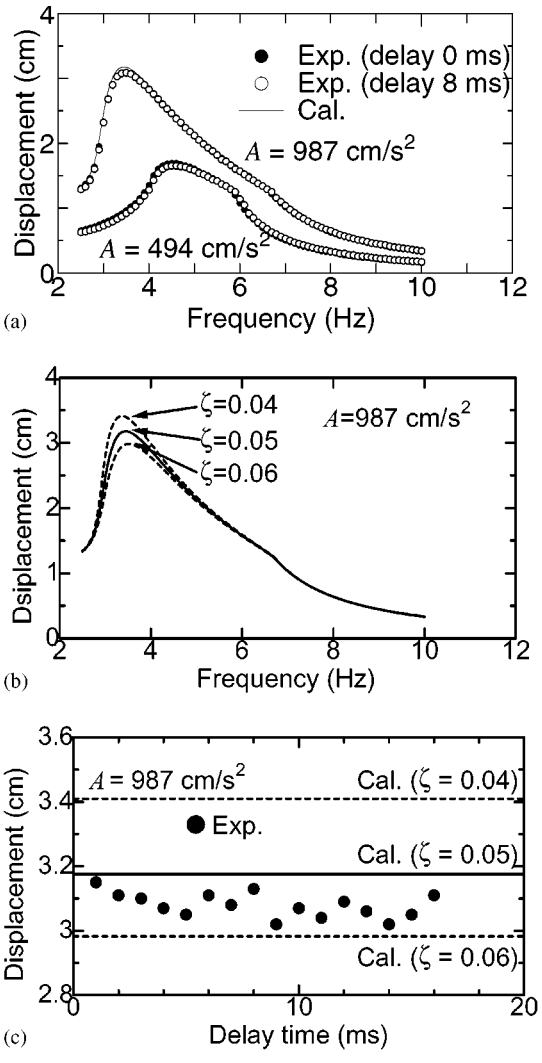

Figure 10. Results of sweep-excitation experiment for bilinear system. (a) Response curve of bilinear system; (b) influence of damping to response curve of bilinear system; (c) maximum response of bilinear system

various damping ratios are shown, larger damping gives smaller amplitude at the resonant region in the bilinear vibration systems but the influence of additional damping is very limited. The maximum amplitudes for various delays under 987-cm/s^2 excitation are also shown in Figure 10(c). The maximum amplitude falls in the damping-ratio range from 0·04 to 0·06 per cent, and this result is consistent with the possible prediction error. The influence of the damping on the bilinear-system response is, however, smaller than that on the linear system as discussed in the above. This is because the dissipated energy caused by the elasto-plastic deformation is large and, therefore, the ratio of damping variation coming from the prediction error to the total dissipated energy in a bilinear system is relatively smaller than that in a linear system.

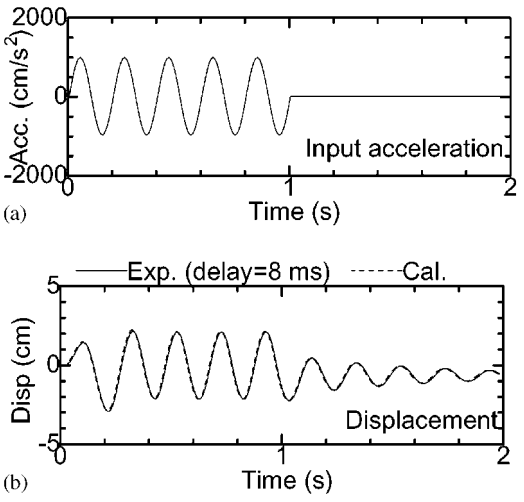

Figure 11. Response time history of bilinear system. (a) Input acceleration; (b) response time history

The displacement response under the 987-cm/s^2 5-Hz and 5-period excitation with a delay of 8 ms is shown in Figure 11. The results including the residual displacement drift are very close to each other. We can therefore conclude that the prediction compensation works well for the bilinear system, too.

5. EXAMPLE OF SEISMIC EXPERIMENTS

5.1. Outline of experiments

Several seismic experiments have been conducted using the developed real-time hybrid experimental system.[8,10] As an example, seismic experiments on a piping system using a new type of support named *energy absorber* are shown in the following.

An Energy Absorber (EAB) is a type of support for piping systems (Figure 12(a)) and it can dissipate vibration energy in the piping system by hysteresis deformation of steel plates contained in it. A series of shaking-table experiments using the simple piping system shown in Figure 12(b) has been conducted to measure the EAB performance.[11] We conducted real-time hybrid experiments for the same structure in order to verify the present experimental method, in which the EAB was actually modelled and the motion of the pipe was simulated by an actuator.

5.2. Hybrid experimental system

The experimental system used here is summarized in Figure 13(a). A digital signal processor was used as a computer because the number of degrees of freedom is small in this numerical model. It should be noted that a computer with more computation power would be necessary if a complex numerical model were required. In such cases, we used a specially developed control computer named *Super Real-time Controller*.[8,12] It can perform large matrix calculations with

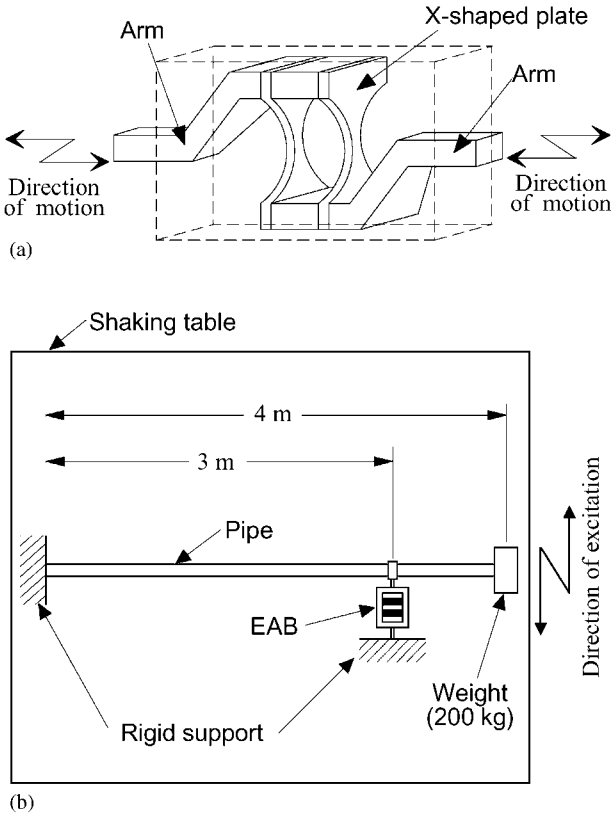

Figure 12. Outline of shaking-table experiment (a) Schematic of EAB; (b) experimental set-up

a small time step as well as communicate with other devices through A/D and D/A converters.

5.3. *Description of experiments*

5.3.1. Energy absorber. As shown in Figure 12(a), the EAB consists of X-shaped steel plates and two rigid arms connected to the pipe and a rigid support. The relative displacement of the arms causes the bending deformation of the X-shaped plates. When the deformation of the plate is relatively large, the elasto-plastic deformation dissipates the vibration energy of the piping system. The plate is X-shaped because this shape makes the bending strain on the plate constant so that the plastic deformation occurs almost all over the plate at the same time. The specifications of the EAB used in these experiments were a load for plastic deformation of 4·9 kN and a maximum allowable displacement of 15 mm. A detailed description of the EAB can be found elsewhere.[11]

5.3.2. Shaking-table experiments. The experimental set-ups are schematically shown in Figure 12(b). The piping model has a length of 4 m, an inner diameter of 78·1 mm, and an outer diameter

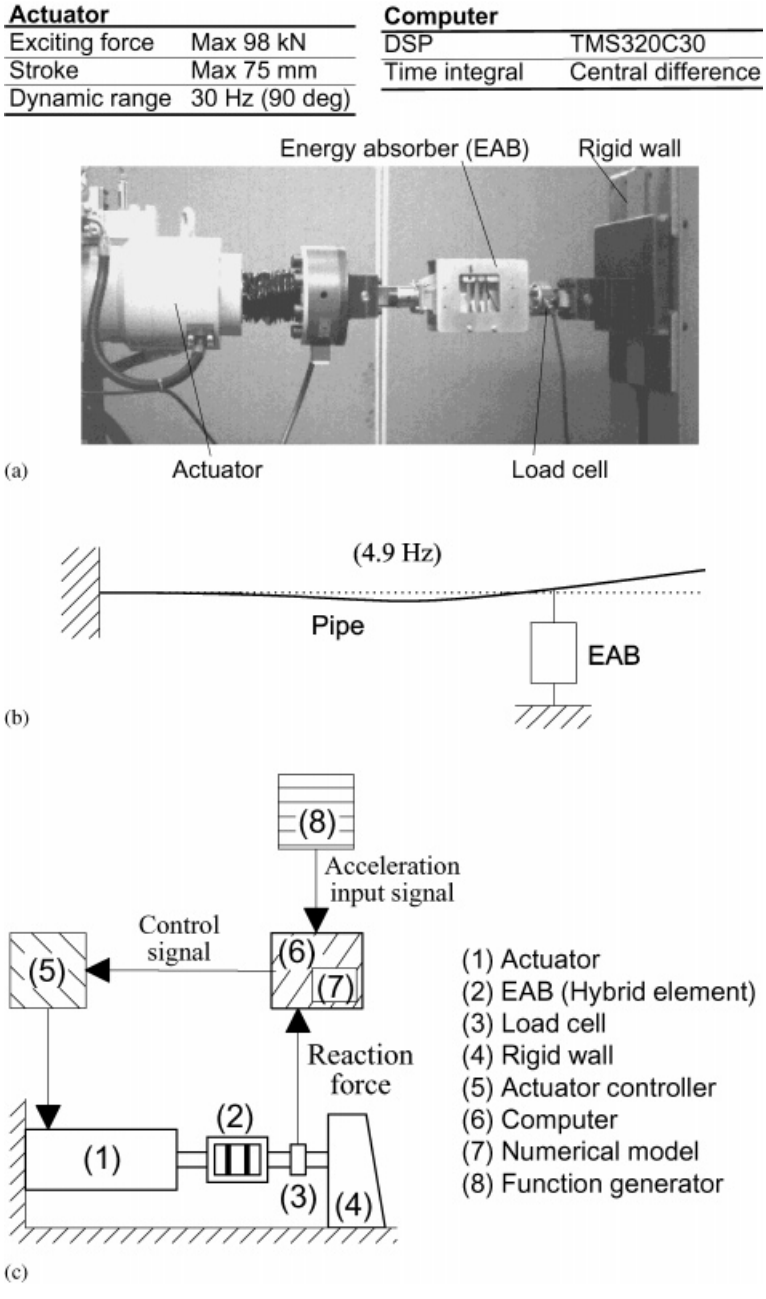

Figure 13. Hybrid experiment for EAB piping systems. (a) Set-up of a hybrid experiment for EAB piping systems; (b) first eigenmode of a piping system supported by EAB; (c) block diagram of the hybrid experiment for EAB piping systems

Table II. Parameter of numerical model of the piping system

Young's modulus	192 (GPa)
Poisson's ratio	0·3
Density	7850 (kg/m^3)
Sectional area	14·45 (cm^2)
Moment of inertia	126·7 (cm^4)
Section modulus	28·44 (cm^3)
Linear stiffness of EAB	2·78 (MN/m)

of 89·1 mm. One end of the model was rigidly supported on the shaking table. At the other end, a weight of 400 kg was attached in order to lower the natural frequency of the model. An EAB supported the piping system so that the distance between the rigid support and the support point of the EAB was 3 m. The model was excited in the direction normal to the axis of the piping model.

5.3.3. Real-time hybrid experiments. Seismic experiments under the same condition as the shaking-table experiments were conducted by making use of the hybrid experimental system shown in Figure 13(a). As the structure under excitation, the EAB was selected. On the other hand, the numerical model consists of 17 nodes and 16 beam elements. The parameters for this model is shown in Table II. In the hybrid experiments here, only the first natural mode (shown in Figure 13(b)) was used in calculation because the other modes have high natural frequencies and therefore are not excited by the acceleration considered. The block diagram of the experiment is shown in Figure 13(c). The control time step for these experiments was 0·5 ms.

5.4. Experimental results

5.4.1. Input acceleration. In the shaking-table experiments, the piping model was excited by using two types of input acceleration: sinusoidal sweep excitation to obtain vibration characteristics; and earthquake excitation to verify the energy dissipation effect of the EAB. As in the shaking-table experiments, the same input acceleration was used for the hybrid experiments.

5.4.2. Sinusoidal sweep excitation. Acceleration transfer functions obtained in the sweep experiments through two experimental methods are shown in Figure 14. In these experiments, the functions using four amplitudes of acceleration from 0·5 to 4 m/s^2 were measured. By comparing two experimental results, similar phenomena can be explained as follows. When the input amplitude is small, a sharp peak is observed near the natural frequency of the piping system. On the other hand, with a larger input amplitude, the maximum amplitude becomes smaller, the sharp peak is diminished, and the frequency giving the maximum response becomes smaller. These phenomena can be explained by the elasto-plastic deformation and the energy dissipation of the EAB. Even though a relatively large discrepancy was found in the small amplitude, the results in the large amplitude and the influence of the input amplitude on the response magnitude, and peak frequencies are almost the same. It should be noted that the discrepancy in the small amplitudes may be caused by gaps at the connections which existed in the shaking-table experiments but were neglected in the hybrid experiments.

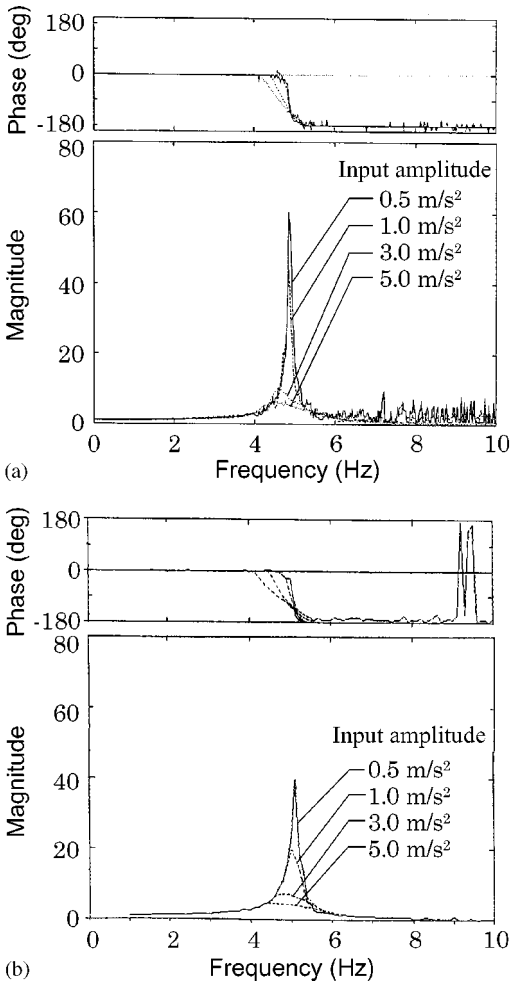

Figure 14. Acceleration transfer functions at the top of the piping system. (a) Hybrid experiment; (b) shaking-table experiment

5.4.3. Earthquake excitation. The acceleration response spectrum of the earthquake used here is shown in Figure 15(a). As shown in this figure, the wave is predominant at 5 Hz, which corresponds with the natural frequency of the piping system under small displacement amplitudes. Time histories of input acceleration, results obtained in the shaking-table experiments, and results obtained in the hybrid experiments, are shown in Figures 15(b), (c) and (d). It can be seen that two experiments gave similar time histories both in displacements and in reaction force. The error in the results occurred because the EABs used in the experiments and the input accelerations were not, strictly speaking, identical in the two experiments. The maximum values obtained in the experiments are compared in Figure 15(e). Both in terms of displacements and reaction force, the two experiments produced similar values.

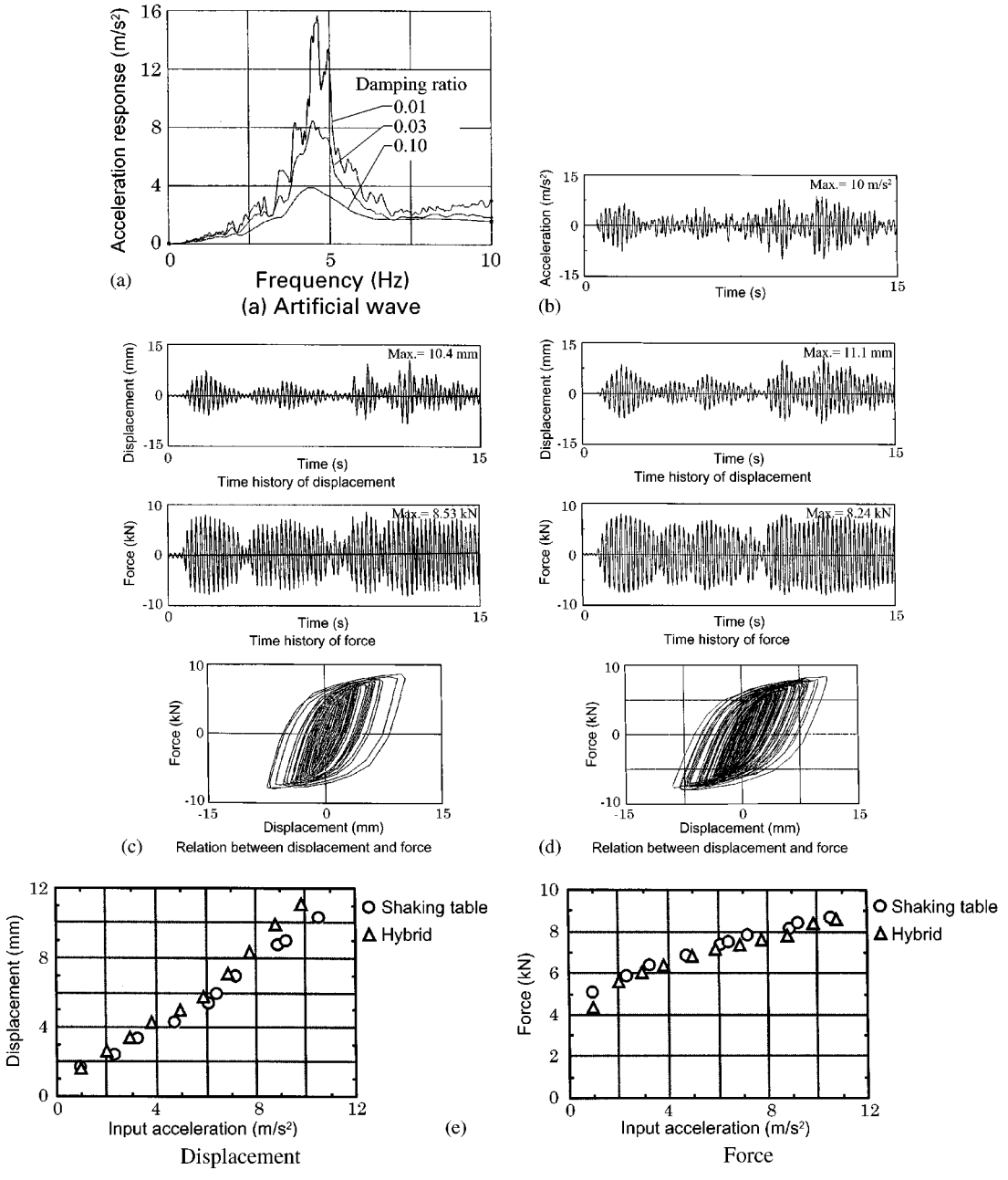

Figure 15. Results of earthquake excitation. (a) Response spectra of input earthquake; (b) time history of input acceleration; (c) time history in shaking-table experiment; (d) time history in hybrid experiment (e) comparison of maximum responses

5.5. Discussions

The experimental results presented show that the two experimental methods (hybrid experiment and shaking-table experiment) gave almost identical results despite small differences. It can therefore be concluded that the structural response can be obtained precisely by using the developed hybrid experimental system. These experiments also showed the advantage of the hybrid experiments, which are simple and economical, because they only require the EAB as the excitation model, while shaking-table experiments need to consider the whole structural system.

6. CONCLUSIONS

Since actuator response delay is equivalent to negative damping in real-time hybrid experiments, a method to cancel out the delay was developed. This method can enable a practical real-time hybrid experimental system to be produced.

The results obtained can be summarized as follows.

- The compensation method to cancel out the actuator delay was developed for real-time hybrid experiments. This method has a stable criterion which depends on the delay time and the excitation frequency. By making use of this developed compensation method, seismic experiments of various types of structures can be conducted when the experimental condition is within this criterion.
- The results of real-time experiments using the developed compensation and those of numerical simulations were compared. These results showed good correlation and therefore the effectiveness of the developed compensation was verified.
- The results of the seismic experiments of a piping system were shown as an example of experiments of actual structural systems. The real-time hybrid experimental system gave close results to those obtained in shaking-table experiments. Therefore the advantages of the hybrid experiments can be demonstrated.

REFERENCES

1. M. Hakuno, M. Shidawara and T. Hara, 'Dynamic destructive test of a cantilever beam controlled by an analog-computer', *Trans. Japan Soc. Civil Engrs* **171**, 1–9 (1969) (in Japanese).
2. H. Iemura, 'Development and future prospect of hybrid experiments', *Trans. Japan Soc. Civil Engrs.* **356**, 1–10 (1985) (in Japanese).
3. K. Takanashi and M. Nakashima, 'Japanese activities on on-line testing', *J. Engng. Mech. ASCE* **113**, 1014–1032 (1987).
4. S. A. Mahin, P-.S. B. Shing, C. R. Thewalt and R. D. Hanson, 'Pseudodynamic test method — current status and future direction', *J. Struct. Engng. ASCE* **115**, 2113–2127 (1989).
5. M. Nakashima, H. Kato and E. Takaoka, 'Development of real-time pseudo dynamic testing', *Earthquake Engng. Struct. Dyn.* **21**, 79–92 (1992).
6. M. Nakagawa, T. Horiuchi, M. Kametani and K. Kikuchi, 'Development of a real-time on-line vibration testing system by substructuring method', *Trans. Japan Soc. Mech. Engrs.* **60**, 412–417 (1994) (in Japanese).
7. T. Horiuchi, M. Nakagawa, M. Sugano and T. Konno, 'Development of a real-time hybrid experimental system with actuator delay compensation (1st report)', *Trans. Japan Soc. Mech. Engrs.* **61**, 1328–1336 (1995) (in Japanese).
8. T. Horiuchi, M. Nakagawa, M. Sugano and T. Konno, 'Development of a real-time hybrid experimental system with actuator delay compensation', *Proc. 11th World Conf. on Earthquake Engineering*, Paper No. 660 (1996).
9. T. Horiuchi, M. Nakagawa, M. Sugano and T. Konno, 'Development of a real-time hybrid experimental system with actuator delay compensation (2nd report)', *Trans. Japan Soc. Mech. Engrs.* **62**, 2563–2570 (1996) (in Japanese).

10. M. Inoue and T. Horiuchi, 'Seismic experiment of FRP columns in a thyristor valve by real-time vibration testing method', *Trans. Japan Soc. Mech. Engrs.* **62**, 1295–1300 (1996) (in Japanese).
11. Y. Namita, J. Kawahata, I. Ichihashi and T. Fukuda, 'Development of seismic design method for piping system supported by elastoplastic damper (2nd report)', *Trans. Japan Soc. Mech. Engrs.* **61**, 3874–3880 (1995) (in Japanese).
12. K. Umekita, M. Kametani and N. Miyake, 'Development of super real-time controller which can perform analysis along with measurement/control in real time', *Proc. 5th Robot Symp. Robotics Society of Japan*, 1995, pp. 55–58 (in Japanese).

